Comparison of a fast low spatial resolution inversion method and peaking factors for the detection of anomalous radiation patterns and disruption prediction

Ivan Wyss [a],[#], Andrea Murari [b], Luca Spolladore [a], Emmanuele Peluso [a], Michela Gelfusa [a], Pasquale Gaudio [a], Riccardo Rossi [a], on-behalf-of-JET-contributors [a],[*]

[a] *University of Rome "Tor Vergata", Via del Politecnico 1, 00133, Rome, Italy*
[b] *Consorzio RFX (CNR, ENEA, INFN, Università di Padova, Acciaierie Venete SpA), Corso Stati Uniti 4, 35127, Padova, Italy*

A R T I C L E I N F O	A B S T R A C T
	The prediction of a disruptive event is a fundamental task for future fusion reactors. On current tokamaks, most remedial actions have the aim of mitigating their effects, but in future machines avoiding such events will be indispensable. As reported in the literature, especially in metallic machines, electron temperature anomalies play a significant role in the destabilisation of MHD modes, leading to disruptions. Plasma radiation has a strong influence on the shape of the electron temperature profile but it is measured by bolometers integrating along viewing cones; therefore tomographic inversion methods are required to obtain local radiation information. Unfortunately, tomographic algorithms are usually slow and not applicable in real-time, implying that they cannot be used for disruption prediction. In this work, we propose a simple, low spatial resolution but fast inversion method that allows calculating the radiation power in the most important regions of the vessel. The method proposed is compared with traditional indicators based on radiation peaking factors. It is shown that, with this fast tomographic algorithm, it is possible to detect and classify anomalous radiation patterns, such as core radiation and MARFEs, and to predict upcoming electron temperature anomalies with much better accuracy and reliability than using simple peaking factors.

1. Introduction

Disruptions are still one of the main challenges in nuclear fusion since future tokamaks need to avoid or at least mitigate all of them, to prevent unsustainable thermal and electromagnetic loads on the plasma facing components and the electromagnetic structures [1–3]. Even a single non-mitigated full plasma current disruption on DEMO could cause unrepairable damage to the machine. On JET, it has been observed that most disruptions are usually due to the destabilisation of MHD modes caused by anomalies in the electron temperature [4,5]. The total radiation emitted by the plasma has a strong impact on the overall shape of the temperature profile. Moreover, anomalies in the radiation emission are typically the earliest precursors, revealing that the configuration is drifting toward an unstable situation. Therefore, developing real-time state observers able to monitor the radiation in the plasma,

with the aim of avoiding such temperature anomalies, is of primary importance especially for avoidance purposes [6,7].Electron temperature anomalies can originate in different regions of the plasma (electron temperature hollowness affects mainly the core, while edge cooling is due to anomaly in the periphery of the plasma) and therefore it is fundamental to monitor the radiation emission in different regions [4,8, 9].

Today, several techniques to monitor the radiation have been developed. The first approach, the most reliable, is the use of tomographic inversion algorithms [10,11].These methods allow measuring the emissivity of the plasma with high spatial resolution, but they are usually limited to post pulse analysis, since their computational time is not compatible with real-time requirements [12]. A deep learning based tomographic reconstruction deployable in real-time has been recently developed and applied to JET [13]. This method works quite well in
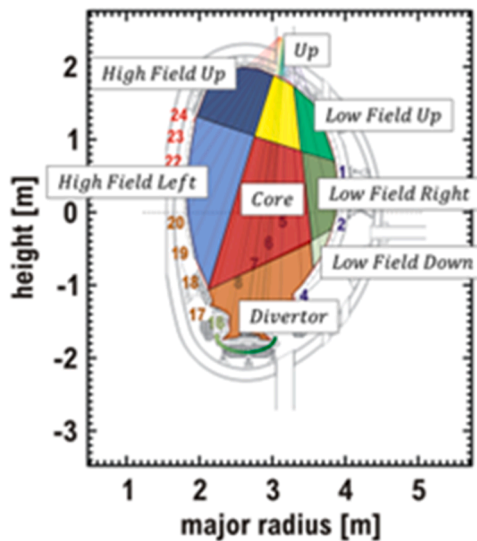
Fig. 1. The eight regions defined for the fast low spatial resolution method.

Fig. 2. Total power emitted by the entire plasma volume calculated with Maximum Likelihood (ML) and fast time resolution inversion(FTRI) for the pulse 94615

standard pulses but, being based on supervised machine learning, it is not the best solution to be used for anomaly detection. Alternatives to tomographic reconstruction, the indicators called peaking factors, have been deployed for many years [9]. These indicators are calculated as the ratio between the core radiation and the total radiation (see next section for details).

This paper analyses a new inversion method, based on low-spatial, high-time resolution reconstruction of the plasma emissivity (and so local radiated power). The new proposed approach allows evaluating the radiated power in the most relevant regions of the plasma cross-section, providing not only the detection of anomalies in the radiation, but also their localisation and classification.

The paper is organised as follows: section 2 introduces the new inversion method and the anomaly indicators. Moreover, it overviews how peaking factors are calculated. In section 3, the indicator behaviours are shown in two disruptive pulses, and then their detection and classification capabilities are assessed with a large set of examples. The conclusions are given in section 4.

2. Methods

2.1. Fast time resolution inversion

From the bolometric cameras, a high spatial resolution reconstruction of the plasma emissivity is obtained through a technique known as tomography. Tomographic algorithms are meant to obtain spatially localised information from external integrated measurements. Given the radiation patterns and the topology of the diagnostic, JET bolometric tomography is a mathematically very ill-posed problem. Its solution requires therefore iterative procedures that cannot be performed in real-time. Decreasing grid resolution allows a fast inversion of the line integrals, even though a lower spatial accuracy is obtained. Nevertheless, by selecting accurately the regions of interest it is possible to maintain sufficient local information. Different regions of interest can be defined by grouping the lines of sight from the horizontal and vertical cameras and intersecting them in the right combinations. Then the inversion is performed by using a nonnegative linear least-squares algorithm. The inversion allows calculating the radiated power in eight regions, called Core, High Field Left (HFL), High Field Up (HFU), Up, Low Field Up (LFU), Low Field Right (LFR), Low Field Down (LFD) and Divertor (see Fig. 1). All these regions are quite important, because excessive radiation in any of them can cause a disruption. However, in the following the attention is focussed on the Core and High Field side Left (HFL), because
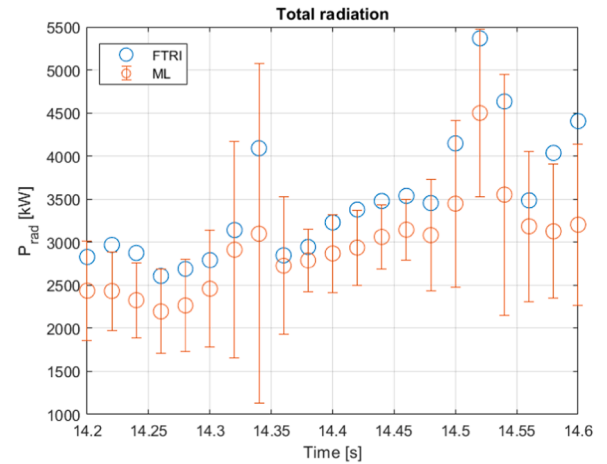
they are essential to detect the two main disruption causes due to excessive radiation emission: heavy impurity accumulation (mainly W) in the core and cooling of the edge (see Subsection 3.1).

In terms of accuracy, the radiation estimated by the fast inversion tomography is typically within 20% of the value calculated with the well-established and validated maximum likelihood approach [14] as shown in Fig. 2.

Moreover, the fast inversion requires a maximum computational time of 50 µs, which is more than adequate since the cycle time of JET real time network is 2 ms. More details about this inversion are reported in [15].

2.2. Anomaly indicators

The determination of the power emitted in each of the eight regions of Fig. 1 is the first step of the procedure to determine the proximity to the radiation stability boundary. Anomaly indicators are also required and have been developed. A good candidate has proved to be the ratio between the radiated power (P_{region}) and the plasma energy (E_{plasma}), which will be indicated as λ_{Region}:

$$\lambda_{Region} = \frac{P_{region}}{E_{plasma}} \tag{1}$$

This indicator is much more informative than the traditional ratio of the radiate power divided by the total input power, which is global and tends to diverge in the ramp down phase of the plasma current, when the additional heating systems are switched off.

To understand the relevance of the λ indicators, one can start by writing the energy Eq. for a region with the barycentre of coordinates ρ and θ:

$$\frac{dE_p(\rho,\theta)}{dt} = P_{in}(\rho,\theta) - P_{rad}(\rho,\theta) + P_t(\rho,\theta) \tag{2}$$

Where P_{in} and P_{rad} are the local input power and radiation emission, while P_t is a term that takes into account all the energy transport phenomena. Dividing by the energy it is possible to write:

$$\frac{1}{E_p}\frac{dE_p(\rho,\theta)}{dt} = \frac{P_{in}(\rho,\theta)}{E_p} - \frac{P_{rad}(\rho,\theta)}{E_p} + \frac{P_t(\rho,\theta)}{E_p} \tag{3}$$

In the case we can neglect P_{in} and transport phenomena, Eq. (4) is obtained:

$$\frac{1}{E_p}\frac{dE_p(\rho,\theta)}{dt} = -\frac{P_{rad}(\rho,\theta)}{E_p} \tag{4}$$
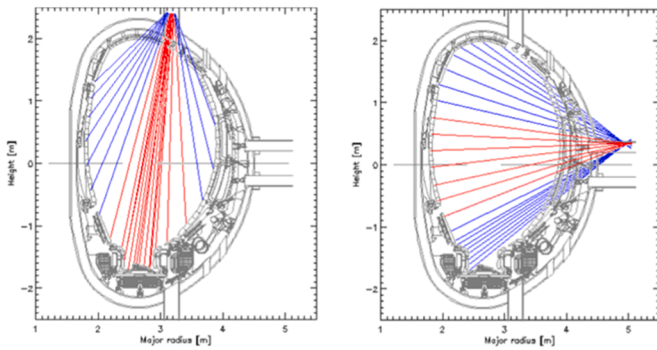
Fig. 3. (Left) Vertical lines of sight of the bolometric camera. (Right) Horizontal lines of sight of the bolometric camera. The red lines are the ones selected for evaluating the peaking factors.

From this last Eq., it is clear how the defined λ indicators are linked to the rapidity of local energy variation, meaning that their value increases when an anomaly is occurring. For example, in the case of electron temperature hollowness, we should expect that not only the radiation is concentrated in the core but also that it is large enough (with respect to the plasma energy) to rapidly cool down the core and lead to the electron temperature anomaly. Normally the λ of the various regions assume values well below 1. When they become larger than unity, it is typically an indication that the radiation is too high and that the situation is becoming dangerous. In any case, the threshold can be optimised for each of the eight regions and for each type of experiment (for example depending on the potential danger for the integrity of the machine of the plasma disrupting).

With regard to the approximations leading to Eq. (4), they are unavoidable because there is no enough knowledge to determine the energy transport and JET does not have a real-time estimator of the input power in the various regions of the plasma cross section. However they are plausible in the proximity to radiation collapses, when the plasma emission is certainly the dominant effect. The good results in term of

predictions, reported in Section 3, tend also to corroborate the assumptions. It is also worth mentioning that the anomalies of the electron temperature profile are measured with the help of specific indicators applied to the measurements of other diagnostics, such as the Thomson scattering or electron cyclotron emission radiometers. These indicators are discussed in full detail in [8].

2.3. Peaking factors

Several peaking factors have been developed in the past to monitor radiation in a tokamak. In this work, the analysis is analogous to the treatment in [9].The peaking factors are defined as the ratio of the mean radiation measured by the bolometric lines of sight around the magnetic axis to the mean over all the lines. In this work, two peaking factors are utilized: one for horizontal lines (Fig. 3, right), PF horizontal, and one for verticals (Fig. 3, left), PF vertical. The choice of the red lines, determining the central region, is empirical, based on experience. However, the results are not very dependent on this choice. Varying the number of central chords within reason does not modify the results appreciably. The two defined peaking factors are also typically the most sensitive for the type of analyses subject of the present work.

3. Results

In the first part of this section, indicators derived from the fast, low spatial resolution tomography are analysed. In particular, the method has been applied to two pulses: 94615 and 96486, to show how representative λ indicators evolve with time. The two discharges are typical examples of radiation anomalies, one causing edge cooling and the other temperature profile hollowness. These are indeed the most significant quantities to illustrate the plasma dynamics for the two most important types of disruption in metallic devices. It is also worth mentioning that in these two cases the current quench starts in the ramp down phase of the plasma current. This is the most common situation on JET but it has been checked that the proposed indicators are equally effective also when the disruptions occur in the flat top of the discharges.
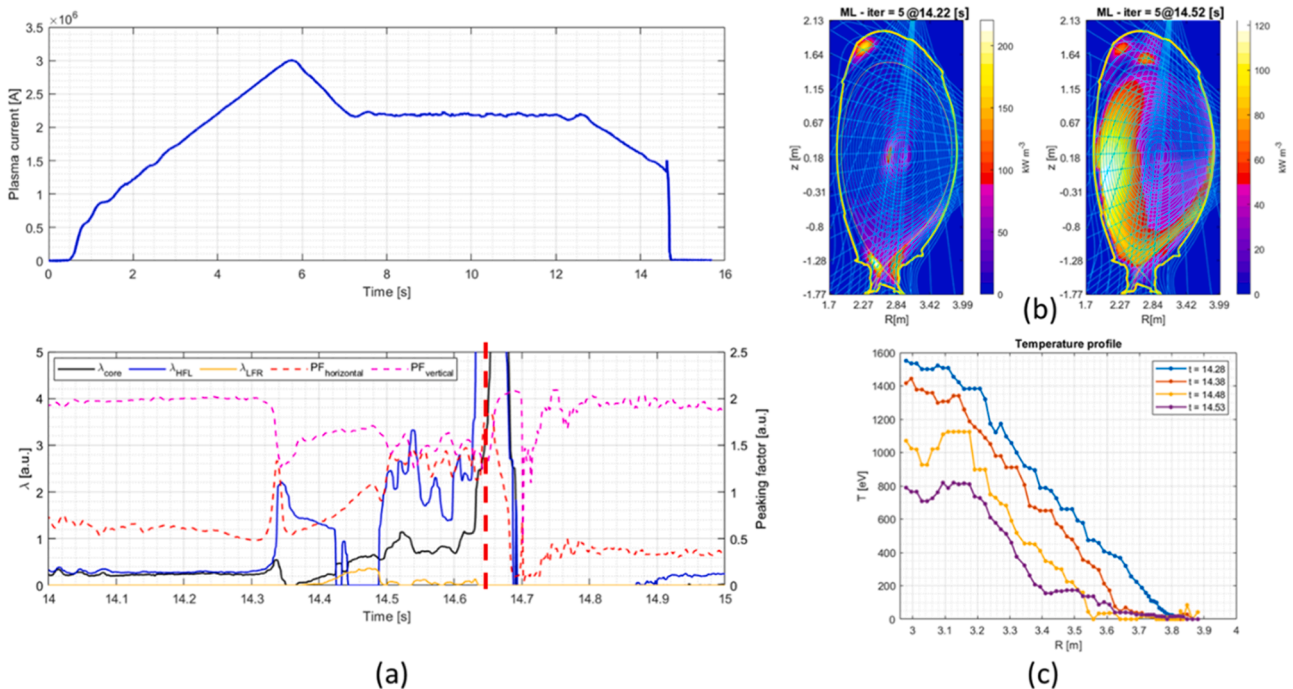

Fig. 4. Pulse 94615 - a): Evolution of the plasma current (top), l indicators and peaking factors in the last hundreds of milliseconds before the disruption (bottom). In the bottom plot the vertical dashed line indicates the beginning of the current quench b):Tomographic reconstructions with the maximum likelihood approach for a time slice before and one after the onset of the MARFE instability. c) Electron temperature profiles from high resolution Thomson scattering before the disruption.
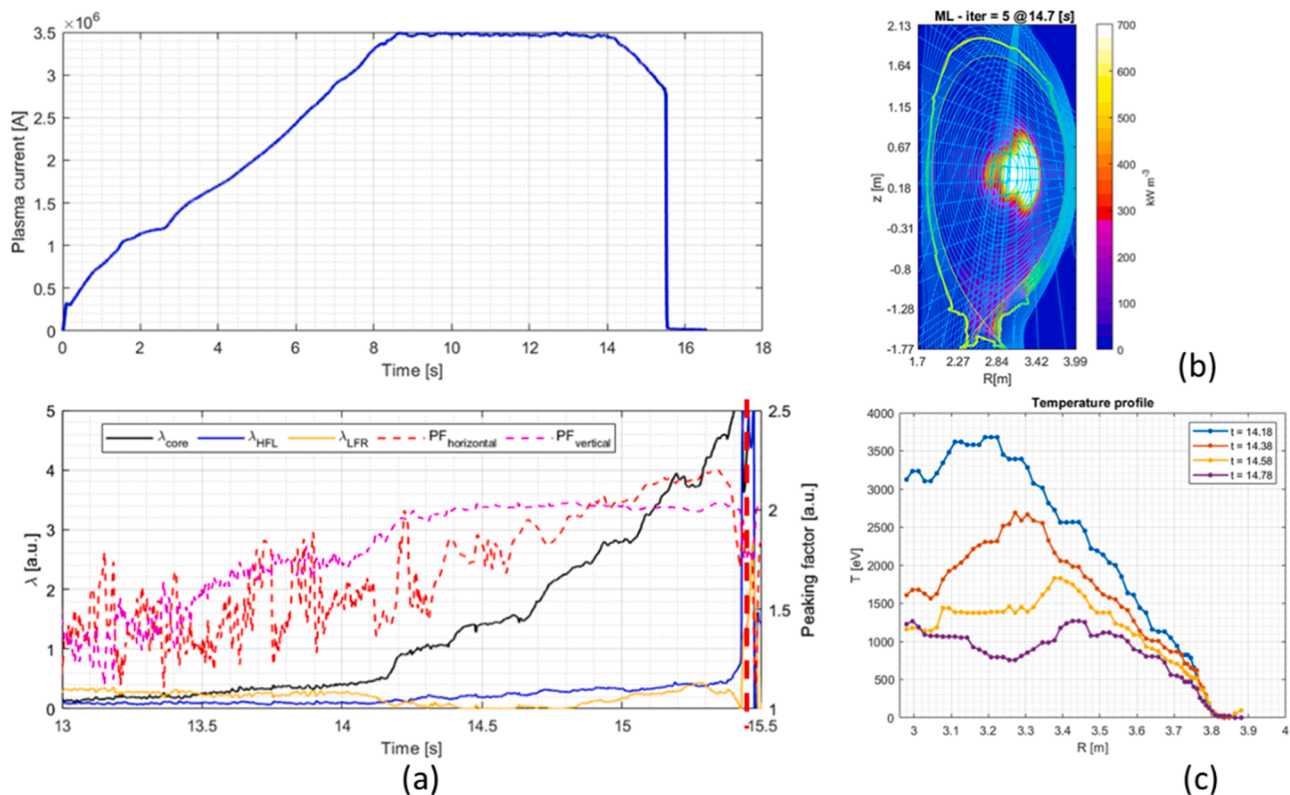
Fig. 5. Pulse 96486 - a): Evolution of the plasma current (top), l indicators and peaking factors in the last hundreds of milliseconds before the disruption (bottom). b): Tomography reconstruction. c) Electron temperature profiles from high resolution Thomson scattering before the disruption. On JET, the electron temperature profile is measured with high spatial and temporal resolution with the Thomson scattering only on the low field side (even if the MARFE appears on the high field side and is therefore detected by the lHFL).

In the second part, the potential of the λ indicators for anomaly detection and classification is illustrated through an analysis of the entire C38 campaign, devoted to the high power deuterium experiments in preparation for the use of tritium. The database consists of 965 pulses, of which 260 are disruptive. The flat top plasma current spans the interval 1.2 MA to 3.5 MA, q_{95} varies between 2.5 and 5.5, while the magnetic field ranges from 1.2 T to 3.8 T and the line integrated electron density between 2 and 8 10^{19} 1/m^3. The maximum core electron temperature was around 7 keV and the maximum neutral beam power about 35 MW. The λ in the core and in the high field left, obtained with the fast low spatial resolution inversion, are the indicators selected for the comparison with the peaking factors: they are the most effective in detecting the radiation anomalies plaguing the two investigated discharges: the edge cooling and the radiation collapse in the core.

3.1. Edge cooling

In pulse 94615, an edge cooling anomaly has occurred (see electron temperature profile in Fig. 4 (c)) leading to a disruption. With the bolometric maximum likelihood tomography (Fig. 4 (b)) the formation of an emitting volume in the high field left region is clearly detected (MARFE anomaly).

Fig. 4 (a) shows how λ_{HFL} rises clearly from 14.32 s, while the level of λ_{core} remains low for much longer. This is exactly the behaviour expected in case of disruptions due to excessive radiation at the plasma periphery and consequent edge cooling. A threshold of about 2 applied to λ_{HFL} would provide a quite good warning time of about 300 ms. It should also be noticed that the drop of λ_{HFL} after 14.4 ms simply indicates that for a while the MARFE moved to a neighbour macro-pixel. Simple inspection of the plots of Fig. 4 reveals also how the peaking factors would be practically useless in this case. Indeed during the

plasma evolution leading to the disruption, they assume values very close to the ones during the stable phase and they start showing anomalous values only after the beginning of the current quench.

3.2. Hollowness

In pulse 96486, a hollowness anomaly occurred (see Fig. 5(c)). From Fig. 5(a), one can see how the λ_{core} increases due to the presence of emission from the core region as observed in the tomographic reconstructions obtained with the Maximum likelihood (ML) algorithm [10]. In the meanwhile, λ_{HFL} and λ_{LFR} increase much later as expected, since the main radiation anomaly is not localised at the edge.

The results show that the indicators based on the fast low spatial resolution inversion produce an alarm when the relative region is effectively emitting an excessive level of radiation. So λ_{core} rises when radiation comes from the core region, indicating a possible hollowness anomaly, while λ_{HFL} and λ_{LFR} increase only much later when also the edge is cooling down excessively. Instead, also in this case the peaking factors remain almost constant for most of the discharge and show signs of problems only much later than the λs. Moreover, although they can sometimes be used to trigger an alarm, the peaking factors do not provide a straightforward interpretation of what region is emitting. Being calculated as the ratios of line integrals, they also lose any information about the intensity of the radiation. Therefore they would need to be complemented by other indicators quantifying the absolute level of the emission.

3.3. Sensitivity and specificity

To determine the performance of the indicators, recourse has been made to the Receiver Operating Characteristic Curve (ROC). The ROC is
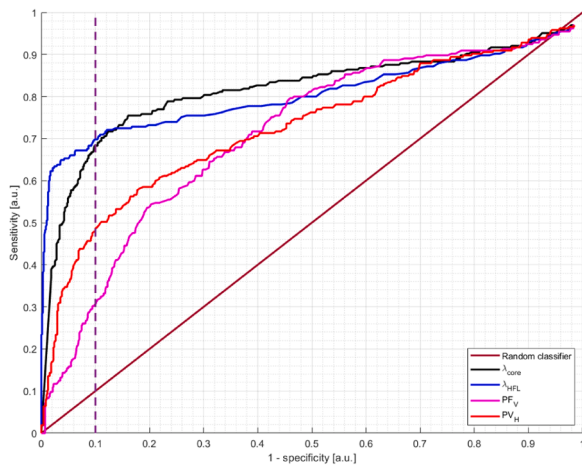
Fig. 6. ROC curves. The superior performance of the l indicators is clear, particularly for realistic values of the false alarms around 10%.

indeed a quite intuitive and consolidated tool to visualise and quantify the diagnostic effectiveness of binary classifiers as their discrimination threshold is varied. It consists of a plot of the sensitivity vs one minus the specificity of the various indicators [16]. The sensitivity is defined as the ratio between true positives and all positives, while specificity indicates the number of true negatives divided by all negatives. Therefore a perfect classifier or indicator would be located in the top left corner of the plot.

In the present application, a true positive means that the indicator triggers an alarm in a disruptive pulse with at least 20 ms before the beginning of the current quench. Indeed 20 ms is an interval more than sufficient for JET control system and actuators to intervene and implement mitigation actions. A true negative is a non-disruptive pulse, in which the indicators have not triggered any alarm. In Fig. 6, the ROC curves are given for the single indicators, i.e. λ_{core}, λ_{HFL}, and both horizontal and vertical peaking factors (alarms are detected by a simple "crossing a threshold" approach). The ROC curves, shown in Fig. 6, have been obtained by scanning the value of the corresponding λ from 0 to 10 with a step of 0.1 (for the peaking factor the range scanned is between 0 and 3 because they have a much smaller dynamic rage). The corresponding numbers of successful detections and false alarms have been calculated for each step and from these values the calculation of sensitivity and specificity is immediate.

The curves prove that the new indicators perform very well (considering that the sensitivity does not reach very high absolute values only because not all the disruptions are due to electron temperature anomalies). Indeed in the C38 campaign there are several pulses that

develop an electron temperature anomaly and recover from it naturally or due to some countermeasures of the control system. The experimental optimal level for one minus the specificity is therefore around 10%. At this value of the x axis, the sensitivity of the new method reaches about the 70%, while the PF method is limited to a value around 50%. An improvement of 20% is statistically very significant and confirms the superior quality of the indicators derived from the fast tomography to the simple peaking factors.

3.4. Classification potential

To understand whether the proposed inversion method can properly determine where the radiation anomalies occur in the cross section, the entire C38 campaign has been analysed with this objective in mind. Comparing the λ indicators with the maximum likelihood tomographic inversions and the videos of the visible cameras, it has been possible to establish that the fats tomography presents very high accuracy; excessive radiation is typically localised exactly in the macro-pixels indicated by the fast tomography. To support this statement for the cases analysed in the present work, two-dimensional histograms in the space $\lambda_{core} - \lambda_{edge}$ have been built for three situations: safe, excessive core radiation and edge cooling (core radiation and edge cooling anomalies are detected by using the methods described in [8]). Then, the histogram counts have been normalised to the sum of all histograms (so that they assume values between 0 and 1) and the results can be observed in Fig. 7.

These maps represent the probability for a measurement to belong to one class. In case of discharges showing a clear blob of radiation in the plasma centre, it is observed that the fast inversion method indicators attribute a high probability to the core radiation (and low to the edge region). On the contrary, when the anomaly is concentrated in low region of the high filed side, the indicators show the opposite combination of values: λ_{HFL} is high whereas λ_{core} remains low.

4. Conclusions

In this paper, a new method to evaluate the local average emissivity and radiated power has been developed and compared with other approaches. The method is fast (50 μs is the maximum inversion time) and deployable in real-time, making it a good candidate to develop state observers to monitor and control the plasma radiation, particularly for avoidance and prevention of radiative collapses. Moreover, new anomaly indicators have been defined starting from simple physical considerations.

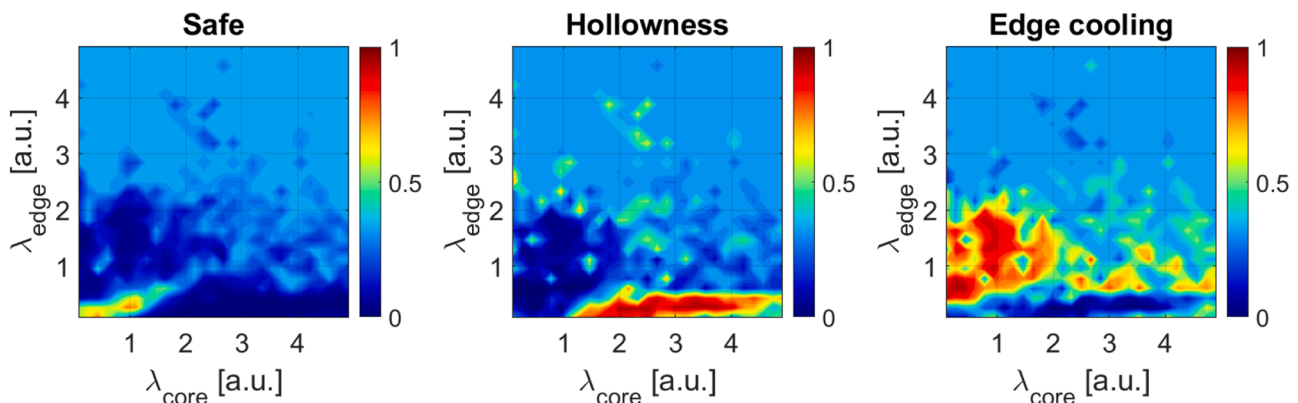The main results support the following conclusions:

Fig. 7. Probability maps of time slices belonging to safe pulses (left), pulses with core anomaly (middle) and edge cooling anomaly (right). These maps have been obtained using the entire database of C38, the last high power campaign before the use of tritium.

- Good agreement between the proposed fast inversion method and the maximum likelihood tomography.
- The indicators, derived from the fast inversion algorithm, have good sensitivity and specificity (good ROC curves) and they may be used as radiation anomaly detectors.
- The developed indicators clearly outperform the traditional peaking factors.
- The indicators developed are able to discriminate between different radiation patterns and can be used to predict what type of electron temperature anomaly is going to occur in the plasma.

Future developments include the implementation of these indicators in general disruption predictors, using both physics and data driven methods (such as machine learning techniques [17–22]). The long term aim of such a line of research would be to obtain an algorithm, capable not only of predicting disruptions but also of detecting and classifying anomalies, to provide the control system with a more comprehensive view of the plasma state, for optimising the feedback solutions.

Declaration of Competing Interest

The authors declare no conflict of interest.

Data availability

Data will be made available on request.

Aknowledgements

References

[1] R. Wenninger et al "Power handling and plasma protection aspects that affect the design of the DEMO divertor and first wall" submitted for publication in Proceedings of 26th IAEA Fusion EnergyConference.

[2] E.J. Strait, et al., Nucl. Fusion 59 (2019), 112012.

[3] T. Hender, et al., Nucl. Fusion 47 (2007) S128–S202, https://doi.org/10.1088/0029-5515/47/6/S03.

[4] G. Pucella, et al., Onset of tearing modes in plasma termination on JET: the role of temperature hollowing and edge cooling, Nucl. Fusion 61 (2021), 046020.

[5] C. Sozzi, et al., Termination of discharges in high performance scenarios in JET, in: 28th IAEA Fusion Energy Conference, 2021.

[6] L. Piron, et al., Progress in preparing real-time control schemes for deuterium-tritium operation in JET, Fusion Eng. Design 166 (2021), 112305.

[7] G. Rattà, et al., Nucl. Fusion 50 (2) (2010), https://doi.org/10.1088/0029-5515/50/2/025005. VolumeNumberJanuary.

[8] R. Rossi et al *"Development of robust indicators for the identification of electron temperature profile anomalies and application to JET"* Plasma Phys. Controlled Fusion, Volume 64, Issue 4, id.045002, https://doi.org/10.1088/1361-6587/ac4d3b.

[9] A. Pau, et al., A first analysis of JET plasma profile-based indicators for disruption prediction and avoidance, IEEE Trans. Plasma Sci. 46 (7) (2018) 2691–2698, https://doi.org/10.1109/TPS.2018.2841394. July.

[10] T. Craciunescu, E. Peluso, A. Muarari, M. Gelfusa, Maximum likelihood bolometric tomography for the determination of the uncertainties in the radiation emission on JET TOKAMAK, Rev. Sci. Instrum.89 89 (5) (2018), 053504, https://doi.org/10.1063/1.5027880, 053504-1-8.

[11] T. Craciunescu, G. Bonheure, V.V. Kiptily, A. Murari, S. Soare, I. Tiseanu, V. Zoitaau, The maximum likelihood reconstruction method for JET neutron tomography, Nuclear Instruments and Methods in Phys. Res. A 595 (2008) 623–630, https://doi.org/10.1016/j.nima.2008.07.145.

[12] R. Mariano et al., Acceleration of an algorithm based on the maximum likelihood bolometric tomography for the determination of uncertainties in the radiation emission on JET using heterogeneous platforms, Appl. Sci. 12 (12) (2022).

[13] A.Matos Francisco, R.Ferreira Diogo, J.Carvalho Pedro, Deep learning for plasma tomography using the bolometer system at JET, Fusion Eng. Design 114 (2017).

[14] A. Murari, E. Peluso, T. Craciunescu, C. Lowry, S. Aleiferis, P. Carvalho, M. Gelfusa, Investigating the thermal stability of highly radiative discharges on JET with a new tomographic method, Nuclear Fusion 60 (12pp) (2020), 046030, https://doi.org/10.1088/1741-4326/ab7536.

[15] R. Rossi et al. "A systematic investigation of radiation collapse for disruption avoidance and prevention on JET" Actually submitted to Nuclear Fusion.

[16] Tom Fawcett, An introduction to ROC analysis" (PDF), Pattern Recogn. Lett. 27 (8) (2006) 861–874, https://doi.org/10.1016/j.patrec.2005.10.010.

[17] J. Vega, A. Murari, S. Dormido-Canto, et al., Disruption prediction with artificial intelligence techniques in tokamak plasmas, Nat. Phys. (2022), https://doi.org/10.1038/s41567-022-01602-2.

[18] A. Murari, et al., Investigating the physics of tokamak global stability with interpretable machine learning tools, Appl. Sci. 10 (2020) 6683.

[19] A. Murari, M. Lungaroni, M. Gelfusa, E. Peluso, J. Vega, JET Contributors, Adaptive learning for disruption prediction in non-stationary conditions, Nuclear Fusion 59 (2019), 086037.

[20] A. Murari, et al., On the transfer of adaptive predictors between different devices for both mitigation and prevention of disruptions, Nuclear Fusion 60 (2020), 056003.

[21] A. Murari, R. Rossi, M. Lungaroni, M. Baruzzo, M. Gelfusa, Stacking of predictors for the automatic classification of disruption types to optimize the control logic, Nucl. Fusion 61 (2021), 036027.

[22] A. Murari, et al., Adaptive predictors based on probabilistic SVM for real-time disruption mitigation on JET, Nuclear Fusion 58 (2018), 056002.